

© 2020 IOP Publishing

Personal use of this material is permitted. Permission from IOP Publishing must be obtained for all other uses, in any current or future media, including reprinting or republishing this material for advertising or promotional purposes, creating new collective works, for resale or redistribution to servers or lists, or reuse of any copyrighted component of this work in other works.

DOI: 10.1088/1748-3190/abc6b3

Bio-Inspired Compact Swarms of Unmanned Aerial Vehicles without Communication and External Localization

Pavel Petráček¹, Viktor Walter, Tomáš Báča, Martin Saska

Department of Cybernetics, Faculty of Electrical Engineering, Czech Technical University in Prague, 166 36, Prague 6, Czech Republic

¹Author to whom any correspondence should be addressed.

E-mail: pavel.petracek@fel.cvut.cz, viktor.walter@fel.cvut.cz, tomas.baca@fel.cvut.cz, martin.saska@fel.cvut.cz

August 2020

Abstract.

This article presents a unique framework for deploying decentralized and infrastructure-independent swarms of homogeneous aerial vehicles in the real world without explicit communication. This is a requirement in swarm research, which anticipates that global knowledge and communication will not scale well with the number of robots. The system architecture proposed in this article employs the UltraViolet Direction And Ranging (UVDAR) technique to directly perceive the local neighborhood for direct mutual localization of swarm members. The technique allows for decentralization and high scalability of swarm systems, such as can be observed in fish schools, bird flocks, or cattle herds. The bio-inspired swarming model that has been developed is suited for real-world deployment of large particle groups in outdoor and indoor environments with obstacles. The collective behavior of the model emerges from a set of local rules based on direct observation of the neighborhood using onboard sensors only. The model is scalable, requires only local perception of agents and the environment, and requires no communication among the agents. Apart from simulated scenarios, the performance and usability of the entire framework is analyzed in several real-world experiments with a fully-decentralized swarm of unmanned aerial vehicles (UAVs) deployed in outdoor conditions. To the best of our knowledge, these experiments are the first deployment of decentralized bio-inspired compact swarms of UAVs without the use of a communication network or shared absolute localization. The entire system is available as open-source at <https://github.com/ctu-mrs>.

Keywords: Swarm Robotics, Relative Localization, Distributed Control, Unmanned Aerial Vehicle

Submitted to: *Bioinspir. Biomim.*

1. Introduction

Use of a team instead of a single robot may yield several general advantages in tasks that either benefit from the multi-robot configuration or are altogether unsolvable by a single robot. The main advantages of robot teams are reduced task execution time, improved robustness, redundancy, fault tolerance, and convenience of cooperative abilities, such as increased precision of measurements with a stochastic element (e.g., localizing ionizing radiation sources [1]), distributing the application payload, and dynamic collaboration (e.g., cooperative object transport [2]).

Deployment of a single UAV requires a complex system composed of several intricate subsystems handling the vehicle control, environment perception, absolute or relative localization, mapping, navigation, and communication. A system scaled to a set of tightly cooperating UAVs must additionally introduce decentralized behavior generation, fault detection, information sharing in an often low-to-none bandwidth communication network, and detection and localization of inter-swarm members. Furthermore, the characteristic environments in the context of aerial swarms suited for real-world challenges may be unknown in advance, they incorporate high density of complex obstacles, they provide none-to-low access to mutual intercommunication between the team agents, and they allow either no access or unreliable access to a global navigation satellite system (GNSS). Each of these concepts is a complex challenge on its own. However, overcoming all the challenges opens the way to applications requiring distributed sensing and acting, such as cooperative area coverage for search & rescue, exploration, or surveillance tasks.

In this article, we present a complete swarm system framework, which respects the swarm and environment characteristics. The properties of the framework presented here correspond closely with the definition of autonomous swarms, as listed in [3]. The properties are: scalability for large groups, high redundancy and fault tolerance, usability in tasks unsolvable by a single robot, and locally limited sensing and communication abilities. Inspired by the self-organizing behavior of large swarms of homogeneous units with limited local information that is found among biological systems, our framework goes even further beyond the swarm requirements from [3] by dealing with all centralized and decentralized

communication with the use of the UVDAR local perception method. The elimination of communication is particularly important in dense swarms of fast-moving aerial vehicles, where time-based delays in mutual localization might disturb the collective behavior of swarms and thus may induce mutual collisions. The independence from communication makes the system also applicable as a backup solution for swarm stabilization in scenarios where communication is required, but suffers from outages.

This allows us to employ a fully decentralized system architecture not limited by scalability constraints. This decentralization is advantageously robust towards a single-point of failure, reduces the hardware demands for individuals, and distributes the sensing and acting properties. We have been inspired mainly by ordinary representatives of biological systems: common starlings *sturnus vulgaris*, which exhibit a remarkable ability to maintain cohesion as a group in highly uncertain environments and with limited, noisy information [4]. Similarly to starlings (and numerous other biological species), the proposed swarming system relies on sensing organs that look on two sides (cameras in our case), observing close-proximity neighbors only and responding to these sensory inputs by a local behavior which together forms a swarm intelligence that reaches beyond the abilities of a single particle.

The UVDAR method tackles the problem of mutual perception of swarm particles by localizing the bearing and the relative 3D position of their artificial ultraviolet (UV) light emission in time, using passive UV-sensitive cameras. The method is deployable in indoor and outdoor environments with no need for mutual communication or for a heavy-weight sensory setup. In addition, it is real-time, low-cost, scalable, and easy to plug into existing swarm systems. To verify the feasibility of the UVDAR technique in an aerial communication-less swarm system, we employed UVDAR to generate a decentralized bio-inspired swarming behavior employing local information about neighboring agents and close-proximity obstacles in real-world conditions. As verified in real-world experiments, the proposed system for relative localization is accurate, robust, and reliable for use in decentralized local-information based swarming models.



Figure 1: A compact aerial swarm of 3 UAVs in a controlled outdoor environment filled with artificial obstacles, as viewed by an outside observer. The decentralized approach, described in detail in section 4, applies a set of local rules contributing to safe navigation and self-organization of the swarm structure among obstacles. The UAVs are homogeneous units with solely local sensing.

1.1. Related Work

1.1.1. Relative Localization

In most recent work concerning swarms and formation flight [5], the proposed algorithms have only been validated either in simulation or in laboratory-like conditions with the presence of absolute localization. This was merely converted to relative measurements virtually, using systems such as real-time kinematic (RTK)-GNSS or Motion capture (mo-cap). It is well known that mo-cap is impractical for real-world deployment of mobile vehicles (either outdoors or indoors), as it requires the installation of an expensive infrastructure. These absolute localization sources can provide the full pose of tracked objects, which oversimplifies the whole task with respect to the reality of practical deployment. Even if only partial information derived from absolute measurements is passed to the UAVs (e.g., distance or bearing), the continuous stream of such information is produced without realistic errors, which is unrepresentative of real-world conditions.

Some more practical approaches consider infrastructure-less sensing such as ranging based on a radio signal [6]. This only allows for distance-based following, without any orientation information, and requires a specific motion for sufficient state observability. Another approach [7], for the 2D case, wirelessly communicates the intentions of the leader. This proves to be feasible since there are fewer degrees of freedom and



Figure 2: Onboard detection of 3 UAVs in the UV spectrum using UVDAR in a member of the aerial swarm. The method directly localizes the neighbors within a swarm in indoor and outdoor environments. Here, the method detects neighbors in an outdoor environment affected by a powerful source of ambient UV radiation. The processing is possible due to periodic blinking of the members with a specific frequency, here with 6 Hz, 15 Hz and 30 Hz.

there is less drift than in a general 3D case. These two approaches rely on radio transmission, which is subject to the effects of network congestion and interference. For this reason, we consider vision-based approaches more suitable for multi-robot groups, especially in uncontrolled outdoor environments.

This approach has previously been explored by the authors' research group, relying on true outdoor relative localization, see [8]. The source of the relative localization was an onboard vision-based system using passive circular markers, as described in [9]. There were, however, drawbacks: high sensitivity to the external lighting conditions and to partial occlusion, and substantial size for an acceptable detection range.

The use of active infrared (IR) markers has also been explored (see [10–12]) for the ability to suppress backgrounds using optical filtering. These methods are however suitable solely for indoor, laboratory-like conditions, since solar radiation excessively pollutes the IR spectrum, and subsequently the signal tends to deteriorate. In [12], the authors employed IR markers with blinking frequency in the kilohertz range, which required event-based cameras to detect micro-scale changes. These cameras are capable of detecting micro-scale changes. However, they typically do not provide sufficiently high field of view and resolution, and they are not suitable for scalable swarms due to their size and cost. The IR spectrum has also been utilized in a passive manner [13], but this approach, though simple, is even less robust to the outdoor conditions

and distances applicable to UAVs.

It is also feasible to visually detect and localize unmarked UAVs using machine learning (ML) methods such as Convolutional Neural Networks (CNNs). However, these approaches require meticulously annotated datasets with a specific UAV and with an environment similar to the intended operational space [14, 15]. The computational complexity and the dependency on satisfactory lighting conditions of such ML systems precludes their deployment onboard lightweight UAVs suitable for swarming. This motivated the development of the UVDAR system, which is more robust to real-world conditions, because it reduces the computational load by optically filtering out visual information that is not of interest. In contrast to [14, 15], UVDAR also provides target identities. The whole sensor is small, lightweight, and does not depend on the external lighting conditions.

1.1.2. System Architecture

To date, deployments of real-world aerial teams have not used any of the methodologies of direct localization described here in order to deal with the mesh-communication between the team members or with the communication link with a centralization element. The record in terms of the number of UAVs cooperating at the same time is currently held by Intel[®] [16] with its fleet of Shooting Star quad-rotors. Intel's centralized solution performs spectacular artistic light shows. However in Intel's arrangement, each team member follows a pre-programmed trajectory, relying on GNSS and a communication link with a ground station. A similar methodology is employed in [17–19], where the authors deployed swarms of UAVs in order to verify bio-inspired flocking behaviors in known confined environments. In comparison with [16], their methods are decentralized; however, the UAVs still communicate their global states obtained by GNSS within a radio-frequency mesh network. This is not a realistic assumption in most application scenarios.

Recent successful real-world deployments are summarized in table 1. Observe that some kind of communication (either ground station to unit or unit-to-unit) is employed in most of the related work. The dependency on a communication network lowers the upper limit for swarm scalability, due to the bandwidth limitations, and significantly reduces the fault tolerance of the entire system. The UVDAR relative visual perception system, described in detail in section 3, is designed to remove this dependency. Its use may allow working swarm systems to mimic the local behavioral mechanisms found in biological systems, ranging from general flocking to leader-follower scenarios.

1.1.3. Swarm Stabilization

To enable short-term stabilization of an autonomous UAV, an onboard inertial measurement unit (IMU) directly measures its linear acceleration, the attitude and the angular rate, using a combination of accelerometers, gyroscopes, and magnetometers. To obtain long-term stabilization of an UAV, however, it is not sufficient to use only the onboard IMU, due to the inevitable measurement noises and drifts. It is common practice to provide an additional estimate of the state vector variables (typically position or velocity), which is fused together with all the inertial measurements. The most common approach is to estimate the global position using a GNSS. However, GNSS signal availability is limited strictly to outdoor environments, and the accuracy of GNSS is affected by an error of up to 5 m [27]. Although the accuracy can be improved to 2 cm with the use of RTK-GNSS, this makes aerial swarms deployable solely in controlled environments and is in contradiction with the biomimicking premise, since precise global localization is uncommon in biological systems. Other common methods of state estimation are local, and they typically employ onboard laser- or vision-based sensors to produce local estimates of the state variables. Vision-based methods may compute the optical flow to estimate the velocity of the camera relative to the projected image plane [28], or may apply algorithms of simultaneous localization and mapping (SLAM) to visual data [29]. Laser-based sensors are mostly used to estimate the relative motion between two frames of generated point-cloud data [30].

There are structurally two approaches for stabilizing a swarm in a decentralized manner. The first group of methods distributes the state estimates determined for individual self-stabilization throughout the swarm (see table 1). In addition to restricting the communication infrastructure, this methodology has a major dependency between the swarm density and the accuracy of the global localization (e.g., GNSS). In addition, it requires knowledge of individual transformations amid the coordination frames for distributed local state estimation methods. The second group of methods does not adopt a communication network to distribute the state estimates, but rather estimates the states directly from the relative onboard observations. This approach makes the swarm independent from the infrastructure, but it makes direct detection, estimation, and decision making with limited information more challenging. As further shown in section 5, the developed framework is part of the second group, perceiving the local neighborhood with visual organs and deploying a swarm of UAVs in fully-decentralized manner.

Work	Decentralized	Communication	Relative localization
<i>Intel</i> [®] [16]	No	Yes*	Shared global position (WiFi)
<i>EHang, Inc.</i> [20]	No	Yes*	Shared global position (WiFi)
<i>Hauert et. al</i> [21]	Yes	Yes	Shared global position (WiFi)
<i>Bürkle et. al</i> [22]	Yes	Yes	Shared global position (WiFi)
<i>Kushleyev et. al</i> [23]	No	Yes*	Shared global position (ZigBee)
<i>Vásárhelyi et. al</i> [17–19]	Yes	Yes	Shared global position (XBee)
<i>Weinstein et. al</i> [24]	No	Yes*	Shared global position (WiFi)
<i>Stirling et. al</i> [25]	Yes	Yes	Infrared (IR) ranging
<i>Nguyen et. al</i> [6]	N/A	Yes	Ultra-Wideband ranging (UWB)
<i>Nägeli et. al</i> [26]	Yes	Yes	Visual markers
This work	Yes	No	UVDAR

Table 1: A brief comparison of aerial swarm systems with successful recent deployments outside of laboratory-like conditions. Methods marked with (*) employ communication with a centralized ground station.

1.1.4. Swarming without Communication

Decentralized swarming models accounting for complete or partial absence of communication were explored exclusively for 2D systems in the past (this is also implied in table 1). The majority of the state-of-the-art works within this field are biologically-inspired and emphasize self-organizing behavior of large-scale swarms of simple units with highly limited sensory capabilities. Highlighted is the Beeclust [31] approach, which uses probabilistic finite state machines and a primitive motion model to mimic the collective behavior of honeybees. The Beeclust can be applied to complex tasks where information exchange among units is not required, such as in underwater exploration using a swarm of underwater robots [32]. A different method [33] analyzes the aggregation of agents towards a common spatial goal while avoiding inter-agent collisions. The authors of [33] show that their method with limited sensing properties of the agents performs similarly to methods employing complete pose information. All of these decentralized algorithms require some form of mutual relative localization (even limited to binary detections), making them suitable for the use of UVDAR localization. Overall review of the 2D approaches is systematically described in [34], which further highlights the lack of research focus in the field of aerial swarming in 3D space.

1.2. Contributions

This article addresses problems of the deployment of real-world aerial swarms with no allowed communication or position sharing. This potential problem is overcome with the use of the novel vision-based UVDAR system for direct mutual perception of team members. The stability of the UVDAR system for use in aerial swarming is the outcome of thorough real-world experimental verification in an outdoor environ-

ment with and without obstacles. The main features of this article are as follows:

- (i) It provides an enabling technology for swarm research, often bio-inspired, by introducing a system that achieves fundamental swarm properties, as defined in [3].
- (ii) It introduces the UVDAR system as an off-the-shelf tool for relative localization and identification of teammates suited for mutual perception of agents in robotic systems, such as aerial swarms.
- (iii) It introduces a decentralized bio-inspired swarming approach suited for obstacle-filled real-world environments, which requires only local relative information and no mutual communication.
- (iv) It verifies the feasibility and analyses the usability of aerial flocking relying on direct localization, which is the most frequent mechanism in biological systems.
- (v) It is based on several real-world deployments of aerial swarms.
- (vi) It presents, to the best of our knowledge, the first autonomous deployments of aerial swarms with no centralized element and no mutual communication.
- (vii) It discloses the entire system as open source at <https://github.com/ctu-mrs>.

2. Motivation

The lack of a communication-independent approach has put a constraint on much of the work done until now in the field of deploying teams of unmanned vehicles in challenging environments. Our work here is motivated by the need for a communication-independent approach, and presents solutions that we have developed. The insights into the development

of the real-world deployments presented here tackle the motivations and constraints of the vast majority of related work restrained by the heretofore lack of communication-independent approaches.

Focusing on dense swarms of UAVs with short mutual distances, most of the swarming approaches reported in the literature have not been tested in real-world conditions. Theoretical derivations, software simulations, and occasional experiments in laboratory conditions have formed the target for most of the related literature, as analyzed in [5] and [35]. However, this research milestone is far away from a meaningful real-world verification needed for an applicability of aerial swarms. Real world interference cannot be neglected, as the integration of a swarming intelligence onto a multi-robot system yields constraints that need to be characterized directly in models of swarming behavior.

Instigated by biologically-inspired swarming models [35, 36] capable of achieving complex tasks (e.g., navigation, cohesion, food scouting, nest guarding, and predator avoidance) with a team of simple units, our aim was to imitate these models with the use of local information, as is widely observed in nature. To allow the deployment of an infrastructure-independent (communication, environment) model, we had identified the most crucial factor impeding this type of deployment of a decentralized architecture – the mutual relative localization between team members, which is also the most crucial information for animals in flocks in nature. This motivated the development of the UVDAR system (see section 3), designed as a light-weight off-the-shelf plugin providing the local localization of neighboring swarm particles. The usability of UVDAR in dense swarms is analyzed in detail in section 6.

3. UVDAR

Inspired by our extensive prior experimental experience with vision-based relative localization of UAVs (see [9, 37]), we developed a novel relative localization sensor that tackles various limitations of previous solutions, namely the unpredictability of outdoor lighting and limits on the size and weight of onboard equipment. The sensor, named *UVDAR*, is a UV vision-based system comprising a UV-sensitive camera and active UV LED markers. These lightweight, unobtrusive markers, attached to extreme points of a target UAV, are seen as unique bright points in the UV camera image (see figure 3). This allows computationally simple detection [38] and yields directly the relative bearing information of each marker from the perspective of the camera. The fish-eye lenses that are used with the UV camera provide a 180° horizontal overview of the surroundings. Known

camera calibration, together with the geometrical layout of the markers on the target, allows us also to retrieve an estimate of the distance (see [38, 39] for details).

In order to provide specific markers that would be distinguishable from others, and also to provide a further increase in robustness with respect to outliers, we set the markers to blink with a specific sequence. Using our specialized implementation of the 3D time-position Hough transform (see [38] for details), we can retrieve this signal for each observed marker, giving them identities. In this project, we use these IDs to simplify the separation of multiple observed neighbor UAVs, but they can also be used to retrieve the relative orientation of the neighbors [39]. In addition to the swarming application described in this paper, UVDAR may be used for e.g., a directed leader-follower flight [39], where the use of the retrieved orientation is essential. In addition, the neighbors' orientation estimate can be exploited for automatic generation of a dataset for training ML vision for UAV detection, as applied in [40], where UVDAR was used for annotating color camera images.

In swarms and in multi-UAV systems in general, the blinking frequency of the onboard LEDs can be configured to encode information for optical data transmission between swarm units, in addition to using LED blinking directly for relative localization. An example of such an application is in exploration, where a scouting unit can indicate the presence and the relative position of a discovered target to other units by combining various blinking signals and the unit's own orientation. A further use is in cooperative voting in a group, where each unit expresses the current selection with blinking signals, and adjusts its vote on the basis of observing the selections of others.

In this paper, we go beyond our preliminary works with UVDAR [38–40], and also beyond other state-of-the-art literature, by incorporating direct mutual localization of UAVs into the position control feedback loop of a fully-decentralized swarming system without any kind of communication and external localization. To the best of our knowledge, this paper presents the first real-world deployments of fully-decentralized bio-inspired swarms of UAVs using direct local localization for collective navigation in an uncontrolled environment. This is what UVDAR was intended for.

3.1. Safety

The use of UV radiation in the system has understandably raised some health concerns in the past. We have verified the safety of this application by consulting the International Commission on Non-Ionizing Radiation Protection (ICNIRP) "Guidelines on limits of exposure



Figure 3: An example of the unprocessed view from the UV-sensitive camera as a part of UVDAR in a member of an aerial swarm. Note the extreme contrast of the LED markers in comparison to the background. A combination of the specific blinking frequency of the LED markers and the high contrast makes them simple to extract from background for processing.

to ultraviolet radiation of wavelengths between 180 nm and 400 nm” [41]. According to these guidelines, the exposure to UV radiation (both to the eyes and to the skin) should not exceed 30 J m^{-2} weighted by the relative spectral effectiveness (unitless wavelength-specific factor). In our case of 395 nm radiation, this factor equals to 0.000036, making the actual limit $8.3 \times 10^5 \text{ J m}^{-2}$. This means that our LEDs, producing 230 mW of total radiated power [42] at the given driving current, can be safely viewed from the distance of 1 m from the frontal direction (with the highest intensity in its Lambertian radiation pattern) for over 3000 h, making it effectively harmless.

3.2. Scalability

In the context of a robotic swarm, scalability of the whole system is an important factor. Using a communication network in large groups of robots limits the scalability by an upper bound defined by the total bandwidth, by the number of available channels, by the network architecture, or by the required data flow. Employing a local perception method such as UVDAR, the state of *swarm particles* (team members, swarm units) is shared via direct observations, as is common in swarms in nature. This system therefore does not need an explicit radio communication network.

As a vision-based method, UVDAR suffers from natural restrictions, namely visual occlusions, camera resolution, and the detection, separation, and

identification of image objects. The upper scalability bound is determined by the ability to filter out the UV markers belonging to a given swarm agent. If the markers of all UAVs in the swarm are set to blink with the same frequency, individual agents have to be distinguished by separating their positions in the UV image and in the constellations that they form. In this case, we estimate that each agent should be capable of distinguishing up to 30 neighboring agents within the range of the UVDAR system, bounded by the computational limitations. This is however not the ideal mode of operation, as it becomes problematic when there are occlusions between agents, or when the agents are in close proximity in the observed image.

To tackle this challenge, we apply different blinking frequencies to different agents. The UVDAR system in its current configuration can accommodate up to 6 different frequencies of blinking that can be reliably distinguished from each other. This allows us to mitigate the issue of overlapping agents - indeed, even agents that are directly behind each other can often be separated, if extreme markers of the further agent protrude into the image. However, since the number of usable blinking frequencies is limited, we need to devise a method for spreading them evenly in the swarm, such that the likelihood of image separation of overlapping agents based on different frequencies between them is maximized for the whole swarm. This has to be done in a decentralized manner, in order not to violate the swarming paradigm.

One way to solve this for dense UAV swarms is to have each agent dynamically re-assign its blinking frequency to differ as much as possible from the neighbors that it observes. This challenge definition can be likewise defined as the constraint satisfaction problem solved within a decentralized swarm of UAVs using direct observations only. The idea of this method is to maximize the local frequency diversity and additionally to allow all of the agents to initiate with the same ID (encoded by the blinking frequency of onboard markers). This opposes the current methodology of manually pre-setting the frequencies before deployment (see section 6). The analysis and the theoretical limits on the convergence of such an approach towards a stable final state maximizing the scalability bound is still underway.

Another approach to increase the scalability bound, while carrying the identical ID on all the agents, lies in the design of UVDAR itself. It is possible to introduce an additional omnidirectional UV source on top of each agent. This additional source is called a *beacon* and it blinks with a specific frequency unique to the rest of the onboard markers on an agent. This allows for the separation of pixels in the image stream based on their image distance as well as their association with the singular beacon marker. The presence of at least two beacons in one region of the observer's image clearly implies a partial mutual occlusion. The use of beacons hence provides a limited ability to separate even agents in partial mutual occlusion relative to an observer if the beacons of both agents are visible.

The maximum range of detection should be taken into account for scalability in the geometrical sense. With the current UVDAR setup, detection is possible for targets up to 15m away from the sensor. However, for improved reliability and robustness, a maximum range of 10m is recommended. For determining the theoretical accuracy and range limitations, see [38]. For a quantitative analysis on real-world accuracy, see section 6.3. Filtering out distant targets, the limited detection range makes the method suitable for dense swarms, which place emphasis on a number of entities in a local neighborhood rather than on the swarm as a whole. In biological systems, this perception characteristic allows for swarms of utmost magnitude, such as fish schools [43] with thousands of entities.

4. Swarming Intelligence

In this article, we follow the swarm concept defined in section 1, in which the group is composed of swarm units with limited computational power and a short-term memory. The concept is decentralized and uses autonomous self-organizing groups of homogeneous

aerial vehicles operating in a 3D space.

The proposed flocking approach works entirely with local information, with no requirement for any form of radio communication between the homogeneous swarm particles, and in an environment with convex obstacles. The approach is inspired by biological systems, where global cooperative behavior can be found to emerge from elementary local interactions. We will show that this phenomenon of cooperative behavior may yield collision-free stabilization in cluttered environments, self-organization of the swarm structure, and an ability to navigate in tasks suited for real UAVs. The proposed swarming framework is founded on previously developed models [44,45], which have been enhanced to suit the demands of real-world interference by extending them with concepts of obstacle avoidance, perception, and navigation. The introduction of such extension concepts is highly important as the assumptions of dimensionless particles and an ideal world as in [44,45] do not apply in the real world. The main idea of the swarming behavior presented here is to verify the feasibility, to perform an analysis, and to derive the properties of the UVDAR system for use in swarm systems. Bear in mind that UVDAR is a general system and any swarming model [17,33,46], formation control approach [47], or obstacle/predator avoidance method [48] utilizing local relative information can be employed to generate intelligent behavior when employing the UVDAR system.

4.1. Behavior Generation

The behavioral model used throughout this article is defined in discrete time step k for a homogeneous swarm unit i with an observation radius $R_n^i \in \mathbb{R}^{>0}$, an obstacle detection radius $R_o^i \in \mathbb{R}^{>0}$, a swarming velocity $\mathbf{v}_{[k]}^i \in \mathbb{R}^{3 \times 1}$, and a set of locally detected neighbors $\mathcal{N}_{[k]}^i$ within the observation radius R_n^i , as follows. Bear in mind that all the relative observations in particle i are given in the body frame of particle i at time step k .

The individual detected neighbor particles $j \in \mathcal{N}_{[k]}^i$ are represented by vectors of relative position $\mathbf{x}_{[k]}^{ij} \in \mathbb{R}^{3 \times 1}$ and relative velocity $\mathbf{v}_{[k]}^{ij} \in \mathbb{R}^{3 \times 1}$, $\forall j \in \{1, \dots, |\mathcal{N}_{[k]}^i|\}$, defined as

$$\mathbf{x}_{[k]}^{ij} = \begin{bmatrix} x_{[k]}^{ij} \\ y_{[k]}^{ij} \\ z_{[k]}^{ij} \end{bmatrix}^T, \quad (1)$$

$$\mathbf{v}_{[k]}^{ij} = \frac{1}{\Delta t_{[k]}^{ij}} \left(\mathbf{x}_{[k]}^{ij} - \mathbf{x}_{[k-1]}^{ij} \right) - \mathbf{v}_{[k-1]}^i, \quad (2)$$

where $x_{[k]}^{ij}, y_{[k]}^{ij}, z_{[k]}^{ij}$ are Cartesian coordinates of a neighbor particle j represented in the body frame of agent i in time step k , $\Delta t_{[k]}^{ij} = t_{[k]}^{ij} - t_{[k-1]}^{ij}$ is the time elapsed since the last direct detection of neighbor j ,

and $\mathbf{v}_{[k=0]}^i = \mathbf{v}_{[k=0]}^{ij} = \mathbf{0}$. The swarming model is then defined as a sum of elementary forces

$$\mathbf{f}_{[k]}^i \left(\mathcal{N}_{[k]}^i, \mathcal{O}_{[k]}^i \right) = \mathbf{f}_{[k]}^{b,i} \left(\mathcal{N}_{[k]}^i \right) + \mathbf{f}_{[k]}^{n,i} \left(\mathcal{N}_{[k]}^i, \mathcal{O}_{[k]}^i \right), \quad (3)$$

where $\mathbf{f}_{[k]}^{b,i}(\cdot) \in \mathbb{R}^{3 \times 1}$ embodies the baseline forces as an interpretation of the *Boids model* [44] flocking rules *cohesion*, *alignment*, and *separation*, modified for real UAVs as

$$\mathbf{f}_{[k]}^{b,i} \left(\mathcal{N}_{[k]}^i \right) = \frac{1}{|\mathcal{N}_{[k]}^i|} \sum_{j=1}^{|\mathcal{N}_{[k]}^i|} \left[\mathbf{x}_{[k]}^{ij} + \frac{\mathbf{v}_{[k]}^{ij}}{\lambda} - \kappa \left(\mathbf{x}_{[k]}^{ij}, R_n^i \right) \mathbf{x}_{[k]}^{ij} \right]. \quad (4)$$

The scalar λ [Hz] is the update rate of direct localization (camera rate) and the weighting function

$$\kappa(\mathbf{x}, r) = \max \left(0, \frac{\sqrt{\|\mathbf{x}\|_2} - \sqrt{r}}{\|\mathbf{x}\|_2} \right) \quad (5)$$

represents a nonlinear weight coefficient scaling the repulsion behavior by the mutual distance between two neighbors. As the original model [44] was designed for swarms of dimensionless particles, function $\kappa(\cdot)$ is particularly important for a swarm of real UAVs, in order to prevent mutual collisions while maintaining flexibility of the swarm as a whole. The force $\mathbf{f}_{[k]}^{n,i}(\mathcal{N}_{[k]}^i, \mathcal{O}_{[k]}^i) \in \mathbb{R}^{3 \times 1}$ in (3) is an extension to the simple model [44] in the form of an additional navigation rule in an environment composed of $\mathcal{N}_{[k]}^i$ and a set of obstacles $\mathcal{O}_{[k]}^i$ detected within the detection radius R_o^i .

The navigation rule can exploit any local multi-robot planning method [49–51] in order to optimize the swarm motion parameters and to prevent a deadlock situation, or can include an obstacle avoidance mechanism and a navigation mechanism by introducing them as additional simplistic rules. To provide an example of the system performance, we introduce a simple attraction force $\mathbf{v}_{[k]}^{n,i} \in \mathbb{R}^{3 \times 1}$ towards a specified goal, together with a local reactive obstacle avoidance rule. To represent the obstacles, we introduce the concept of a *virtual swarm particle*, which efficiently replaces a general geometric obstacle by a virtual entity. This dimensionless particle is represented by a state comprised of a position and velocity relative to particle i , similarly as defined in (1) and (2). The methodology for finding the state of a virtual swarm particle is derived in the following section. The navigation rule is then derived as

$$\mathbf{f}_{[k]}^{n,i} \left(\mathcal{O}_{[k]}^i \right) = \frac{1}{|\mathcal{O}_{[k]}^i|} \sum_{v=1}^{|\mathcal{O}_{[k]}^i|} \left[\frac{\mathbf{v}_{[k]}^{iv}}{\lambda} - \kappa \left(\mathbf{x}_{[k]}^{iv}, R_o^i \right) \mathbf{x}_{[k]}^{iv} \right] + \frac{\mathbf{v}_{[k]}^{n,i}}{\lambda}, \quad (6)$$

where the vectors of the relative position $\mathbf{x}_{[k]}^{iv} \in \mathbb{R}^{3 \times 1}$ and the relative velocity $\mathbf{v}_{[k]}^{iv} \in \mathbb{R}^{3 \times 1}$ constitute the state of a v -th virtual swarm particle.

The swarming model defined in (3) represents the steering force of a particle i , which is used to compute the swarming velocity of particle i as

$$\mathbf{v}_{[k]}^i = \gamma \left(\mathbf{f}_{[k]}^i \left(\mathcal{N}_{[k]}^i, \mathcal{O}_{[k]}^i \right) \right) \frac{\mathbf{f}_{[k]}^i \left(\mathcal{N}_{[k]}^i, \mathcal{O}_{[k]}^i \right)}{\left\| \mathbf{f}_{[k]}^i \left(\mathcal{N}_{[k]}^i, \mathcal{O}_{[k]}^i \right) \right\|_2}, \quad (7)$$

where

$$\gamma(\mathbf{f}) = \min \{ v_m; \lambda \|\mathbf{f}\|_2 \} \quad (8)$$

bounds the magnitude of the velocity below the maximum allowed speed v_m [m s⁻¹]. The swarming velocity is then used in real-world applications to compute the desired position setpoint as

$$\mathbf{r}_{[k]}^{d,i} = \frac{\mathbf{v}_{[k]}^i}{\lambda} \quad (9)$$

represented in the body frame of UAV i .

4.2. Obstacle Detection

To achieve flocking in the targeted environment (e.g., a forest environment and an indoor environment), the obstacles in the local neighborhood are generalized into two geometrical classes (circles and lines), based on their cross-sections with the horizontal plane of a particle, as portrayed in figure 4. This assumption allows us to model more complex settings (e.g., a forest or an office-like environment) on the grounds of these two geometrical classes, while it throttles down the perception and the computational complexity onboard a lightweight UAV. Detection of these obstacles is assumed to be provided for a particle i from any kind of an onboard sensor with an obstacle detection distance R_o^i .

Having in time step k a detected circular obstacle v with a radius $r_{[k]}^v \in \mathbb{R}^{>0}$ and a center at $\mathbf{c}_{[k]}^{iv} \in \mathbb{R}^{3 \times 1}$ referenced in the body frame of particle i , the state of a v -th virtual swarm particle is derived as

$$\mathbf{x}_{[k]}^{iv} = \left(1 - \frac{r_{[k]}^v}{\|\mathbf{c}_{[k]}^{iv}\|_2} \right) \mathbf{c}_{[k]}^{iv}, \quad (10)$$

$$\mathbf{v}_{[k]}^{iv} = \frac{r_{[k]}^v}{\|\mathbf{c}_{[k]}^{iv}\|_2} \left(\mathbf{I} - \boldsymbol{\mu}_{[k]}^{iv} \left(\boldsymbol{\mu}_{[k]}^{iv} \right)^T \right) \mathbf{v}_{[k]}^i, \quad (11)$$

where $\|\cdot\|_2$ is the L² norm, $\mathbf{I} \in \mathbb{R}^{3 \times 3}$ is an identity matrix, and $\boldsymbol{\mu}^{iv} = \frac{\mathbf{c}^{iv}}{\|\mathbf{c}^{iv}\|_2}$. By analogy, the virtual swarm agent state can be derived for a linear obstacle defined by its normal vector $\mathbf{n}_{[k]}^{iv} \in \mathbb{R}^{3 \times 1}$ and a set of

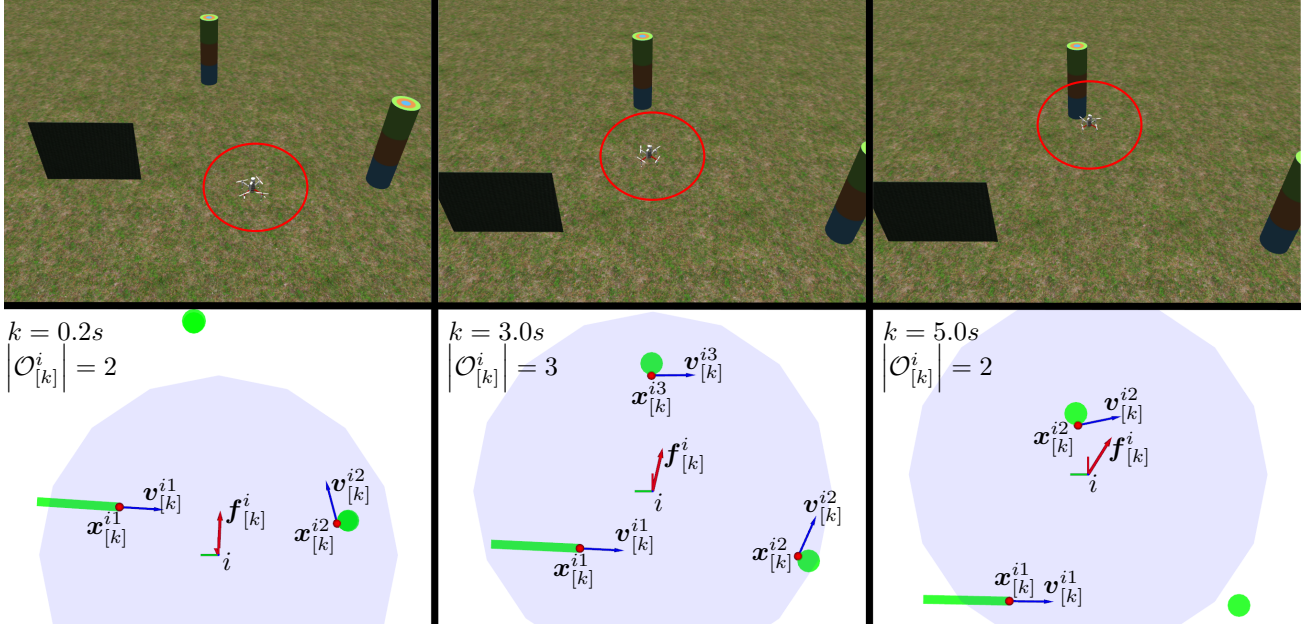


Figure 4: An autonomous UAV navigating among artificial obstacles according to the swarming model described in section 4. The UAV flies in the Gazebo robotic simulator (upper row), while it continuously detects geometrical obstacles represented as circles and lines in the onboard 2D laser-scanner data with a limited obstacle detection radius (gray circle). The states of virtual particles, consisting of position $\mathbf{x}_{[k]}^{iv}$ (red dots) and velocity $\mathbf{v}_{[k]}^{iv}$ (blue arrows) relative to UAV i , are visualized in the bottom image row. The steering force $\mathbf{f}_{[k]}^i$ (red arrow) of the swarming model represents the desired velocity.

observed points $\mathcal{P}_{[k]}^{iv}$ as

$$\mathbf{x}_{[k]}^{iv} = (\mathbf{I} - \mathbf{P}_{[k]}^{iv}) \hat{\mathbf{p}}_{[k]}^{iv} \quad (12)$$

$$\mathbf{v}_{[k]}^{iv} = \frac{1}{\|\hat{\mathbf{p}}_{[k]}^{iv}\|_2} \mathbf{P}_{[k]}^{iv} \mathbf{v}_{[k]}^i, \quad (13)$$

where

$$\mathbf{P}_{[k]}^{iv} = \mathbf{I} - \mathbf{n}_{[k]}^{iv} \left(\mathbf{n}_{[k]}^{iv} \right)^T, \quad (14)$$

$$\hat{\mathbf{p}}_{[k]}^{iv} = \arg \min_{\mathbf{p} \in \mathcal{P}_{[k]}^{iv}} \{\|\mathbf{p}\|_2\}. \quad (15)$$

The state of a virtual swarm particle for both geometrical classes is visualized in figure 4, where an autonomous UAV navigates among artificial obstacles within an environment of the Gazebo robotic simulator.

5. System Architecture

In addition to the method for direct onboard localization presented in section 3 and the decentralized swarming approach presented in section 4, we will now present here system architecture of the entire UAV system, supplemented by the concepts of UAV stabilization, control, and state estimation. These concepts

are based on our previous research (see [1, 37, 52]) focused on cooperation among autonomous aerial vehicles. They have been adapted for swarming research described in this article. The control pipeline, suited for stabilizing and controlling UAV swarms using linear model predictive control (MPC) and the non-linear SO(3) state feedback controller [53], is depicted in the high-level scheme in figure 5. The stabilization and control pipeline is based entirely on [52].

In addition, a decentralized collision avoidance system [55] is adapted in the proposed system for safe research on compact aerial swarms. A long prediction horizon of linear MPC is used to detect collisions among trajectories of robots. The known collision trajectories are then altered prior their execution. This allows us to implement the collision avoidance system in a decentralized manner. Decentralized collision avoidance is necessary for safe verification of bio-inspired swarming models in the real world. Although the use of mutual communication for collision avoidance is in contradiction with the system architecture presented in this article, it can be used as a low-level safety supervisor with no direct dependency on the architecture of the tested swarming model. This may prevent inadmissible collisions when there is undesired demeanor of dense swarm members, and therefore protect the hardware during the initial phases

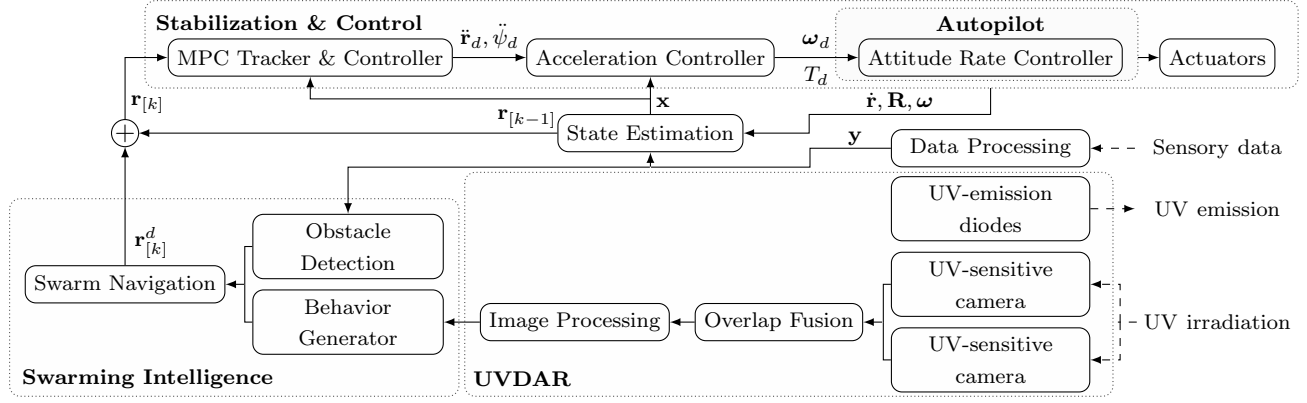


Figure 5: The high-level system pipeline (the schematic is based on the system pipeline diagram published in [54]) of a single homogeneous UAV swarm unit i in time step k . The stabilization & control pipeline [52] takes reference position setpoint $\mathbf{r}_{[k]}$ for the MPC in the MPC tracker, which outputs a command $\ddot{\mathbf{r}}_d, \ddot{\psi}_d$ (ψ is the heading acceleration) for the acceleration tracking SO(3) controller [53]. The acceleration controller produces the desired angular rate $\boldsymbol{\omega}_d$ and thrust reference T_d for the embedded attitude rate controller. A state estimation pipeline outputs the current state estimate \mathbf{x} based on the sensory data \mathbf{y} and the onboard measurements of linear velocity $\dot{\mathbf{r}}$, angular rate $\boldsymbol{\omega}$, and attitude \mathbf{R} . Note that the time indices of the stabilization & control and the state estimation pipelines are omitted in the diagram, since their timeline matches the rate of the inertial measurements (typically 100 Hz), which differs from the timeline of the detection cameras (10–20 Hz). Local perception of neighboring units using the UVDAR sensor is described in detail in section 3, while the decentralized swarming approach is described thoroughly in section 4.

of experimental swarm deployment. However, the use of collision avoidance is not mandatory and its use is appropriate only during the initial testing phase.

To stabilize UAVs using the system in figure 5, the individual UAVs estimate their state vector

$$\mathbf{x} = [\mathbf{r}, \dot{\mathbf{r}}, \ddot{\mathbf{r}}, \mathbf{R}, \boldsymbol{\omega}]^T, \quad (16)$$

where $\mathbf{R} \in \text{SO}(3)$ is the attitude and $\mathbf{r} = [x_w, y_w, z_w]^T$ is the position in the world coordinate frame. The vector $\dot{\mathbf{r}} \in \mathbb{R}^{3 \times 1}$ is the linear velocity, $\ddot{\mathbf{r}} \in \mathbb{R}^{3 \times 1}$ is the linear acceleration, and $\boldsymbol{\omega} \in \mathbb{R}^{3 \times 1}$ is the angular rate with respect to the UAV body coordinate frame. The PixHawk autopilot [56] is embedded to handle the low-level attitude rate and actuator control, and an IMU is used to directly measure the linear acceleration $\ddot{\mathbf{r}}$, the attitude \mathbf{R} , and the angular rate $\boldsymbol{\omega}$, using a combination of accelerometers, gyroscopes, and magnetometers. The embedded autopilot integrates the measurements of $\ddot{\mathbf{r}}$ to $\dot{\mathbf{r}}$ and employs the Extended Kalman Filter (EKF) to produce optimal estimates of the specific state variables with respect to the measurement noise.

To self-localize an individual UAV, its global position measured by GNSS is fused together with the inertial measurements in order to stabilize the flight of this dynamically unstable system. However, the global state is not shared to other swarm agents throughout our final experimental analysis presented in section 6. Instead, the framework uses UVDAR to directly observe the relative position and the relative velocity (see (1) and (2)) of particles in the

local neighborhood, and it generates a navigation decision based on the set of simple rules described in section 4. Although the use of GNSS for self-localization limits the system exclusively to outdoor environments, this dependency can be replaced by any local state estimation method with respect to the desired application and environment – e.g., the deployment of our decentralized system in a real-world forest, which was highlighted by the IEEE Spectrum ‡.

5.1. Properties

The combination of the system decentralization and the local perception of individual agents makes the system as a whole robust towards failures of individuals. In the swarming model (see section 4), each agent decides on its actions in real time only from current observations or a short-past history of observations. This makes the system robust towards a single-point of failure, such as a failure of some centralized control element or the communication infrastructure. Unless the employed local perception method generates false negative detections, the swarming model (see section 4) ensures no mutual collisions between the agents. The rate of false negative detections in UVDAR is minimal as there are no objects blinking at specific rates in the given near-visible UV spectrum. In case of a hardware failure of an aerial agent (e.g., the agent lands unexpectedly), the

‡ <https://spectrum.ieee.org/automaton/robotics/drones/video-friday-dji-mavic-mini-palm-sized-foldable-drone>

agent disappears from the visibility field of other units resulting in emergent self-organization of the collective configuration.

As UVDAR is a vision-based system, it naturally suffers from visual occlusions generating blind spots in overcrowded situations. As discussed in section 3.2, the number of visual occlusions in UVDAR is mitigated with the use of different blinking frequencies of overlapping UAVs. As the neighborhood for perception is also locally limited in the swarming model (see section 4), the distant blind spots are filtered out in principle. The remaining occluded agents are neglected. This is feasible in the employed model, as the information about the units' presence is propagated through direct observations of the motion of the middle agents (i.e., the agents causing the occlusions). Based on our empirical experience, this does not destabilize the swarm, but rather rearranges the agents to positions where the number of visual occlusions is reduced.

The navigational features of the system as a whole are controlled in a decentralized manner. A decentralized navigation is possible with a swarming model capable of navigational decision making using only the perceived data onboard the units. This is the case of our swarming model (see section 4), which employs a simple steering towards a pre-specified set of global positions, hence eliminating the need for navigation managed by a centralized controller. Although our later experiments (see section 6) navigate each UAV individually, the model may navigate only a single unit with the rest of the swarm naturally following the leader – a behavior emerging from the cohesion and the alignment premises.

5.2. Hardware Platform

The use of UVDAR is not dependent on the dimensions or the configuration of a multi-rotor platform. The payload (onboard equipment) requirements of a single-UAV unit employing UVDAR are: an autopilot, a self-localization source (e.g., a GNSS receiver), 1-2 UV-sensitive cameras, computational power to control the flight and to process the data (one camera at 20 Hz requires approximately a 30% single-thread load on Intel-Core i7 7567U, 3.5 GHz), and a set of UV LED markers placed at known extreme points of the UAV.

To verify this statement, an axiomatic functionality validation of UVDAR was performed on two independent multi-rotor platforms as shown in figure 6. The general hardware configuration of UAVs exhibited in the figure consists of

- the Pixhawk 4 autopilot,
- onboard computer Intel NUC i7 7567U,

- *ProLight Opto PM2B-1LLE* near-UV LEDs radiating at 390–410 nm wavelength [42],
- *mvBlueFOX-MLC* cameras with
 - a *MidOpt BP365* near-UV band-pass filter and
 - *Sunnex DSL215* fish-eye lenses,
- a GNSS receiver (the hexa-rotor platform only), and
- the Slamtec RPLiDAR-A3 laser scanner (the quad-rotor platform only).

The weight of this hardware configuration is 370 g (or 540 g with the laser scanner required either for an obstacle detection or for a local localization replacing the GNSS dependency). The onboard Intel NUC computer weighing 225 g provides exaggerated processing power useful particularly in our case for general research purposes. For use in highly specialized applications, a feasible replacement of this payload with a microprocessor technology would allow for even further minimization of the aerial platform dimensions and cost expenses.

Further miniaturization of infrastructure-independent UAVs is limited by current technology required for local self-localization. Vision-based algorithms employ lightweight cameras minimizing the weight; however, it comes at the cost of high processing power and thus increased weight of the processing unit. On the other hand, laser-based localization generally requires less processing power, but the sensors are heavier than cameras – approximately 170 g for planar scanners and 475 g for 3D LiDARs.

6. Experimental Analysis

The primary aim of the experimental analysis is to verify the general functionality and to evaluate the performance of the entire framework exploiting direct localization rather than communication. The objectives of the experiments are focused primarily on determining the accuracy of the UVDAR direct localization, and on the stabilization and spatial navigation of an aerial swarm in real-world environments with and without obstacles. The entire experimental analysis is supported by multimedia materials available at <http://mrs.felk.cvut.cz/research/swarm-robotics>.

6.1. Swarming Model Analysis

To rule out the influence of UVDAR in a position control feedback loop of an aerial swarm, the *Boids*-based swarming intelligence (see section 4) is analyzed independently from the direct localization. For this purpose, the UAVs replace direct visual localization by sharing their global GNSS positions in an ad-hoc network in order to determine the relative arrangement

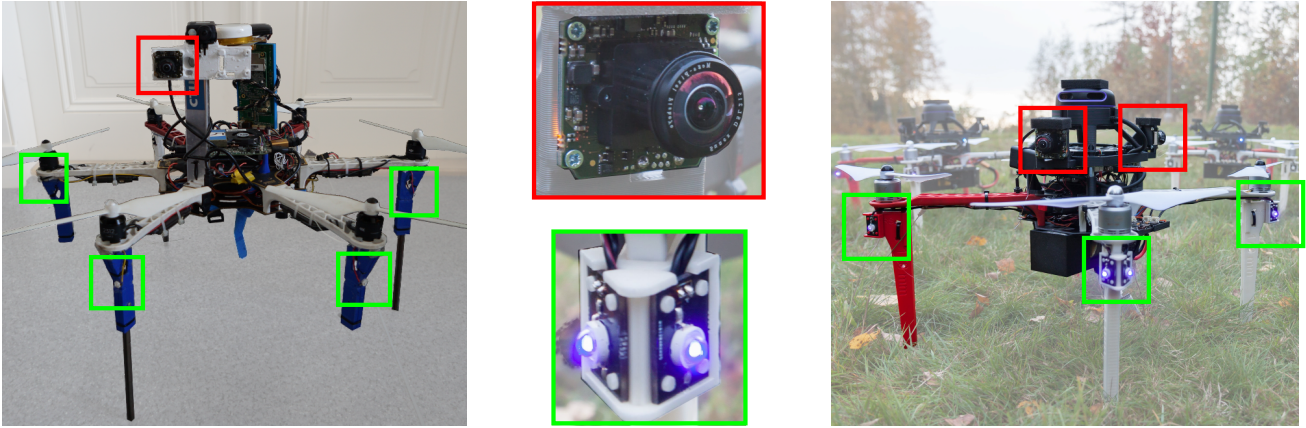


Figure 6: Two distinct multi-rotor (hexa- and quad-rotor) UAV platforms, here equipped with UV-sensitive cameras (red) and with active UV markers (green), comprising the hardware components of the UVDAR system for relative localization of neighboring UAVs. The diagonal dimension (without propellers) of the platforms are 550 mm (left) and 450 mm (right). The hexa-rotor platform was used throughout our experimental verification presented in section 6.

in the local neighborhood. This configuration was necessary in order to deploy UAVs without direct localization using UVDAR, as discussed in section 1.1. The analysis showcases the usability of the proposed fully-decentralized swarming framework both in simulations and in real-world scenarios, and in environments with and without obstacles. The global positions of the obstacles are a priori available to the UAVs.

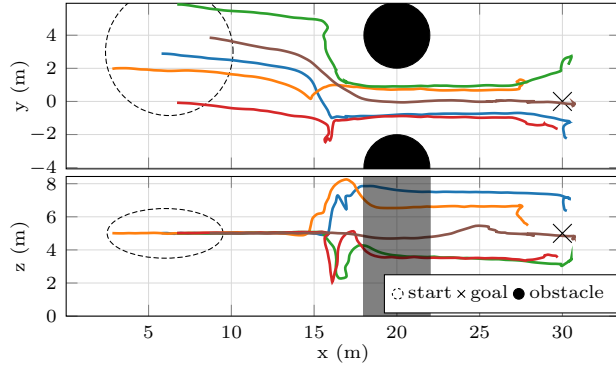
First, the collective dynamics of the swarming model are analyzed thoroughly in the Gazebo robotic simulator [57], shown in figure 4, coupled with the Robot Operating System (ROS) [58]. This simulation environment emulates real-world physics, and allows us to use identical low-level controllers and state estimation methods (see section 5) for the real UAVs and also for the simulated UAVs, without simplifying assumptions. This makes the configuration ideal for effortless deployment of theoretical bio-inspired swarming approaches onto a group of real-world robots. Simulation deployment of a swarm of homogeneous units in a 3D environment with obstacles (see figure 7) verifies the qualitative performance of the reactive obstacle avoidance methodology presented in section 4. The emerging collective dynamics show the properties of the 3D shape flexibility during navigation through a narrow passage and in collision-free bypassing of static obstacles. The properties of safe navigation and high flexibility are also showcased during the simulation deployment of a compact swarm of 9 homogeneous units in a dense 3D forest-like environment, according to figure 8.

Second, an aerial swarm of 3 UAVs was experimentally deployed in a real-world forest-like

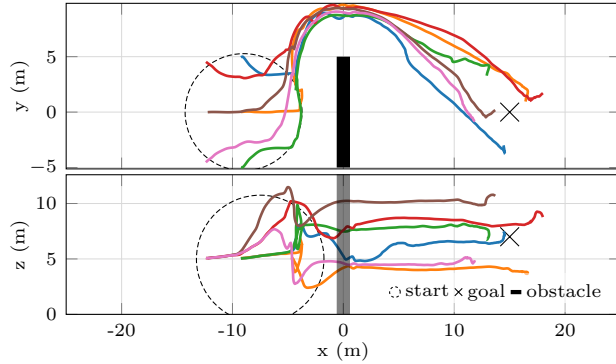
environment similar to figure 8, in order to verify the abilities of the fully-decentralized swarming model to stabilize a set of UAVs in a decentralized manner, provide self-organizing behavior, and to navigate through an obstacle-filled environment. As explicitly shown in figure 9, even such a simplistic swarming model with only local information yields collision-free navigation (the minimum distance to an obstacle or to another UAV was 2.2 m) throughout the environment, and self-organizing compactness of the whole swarm during the entire flight. The experiment likewise shows the ability of the model to divide the group when overcoming an obstacle and to unite back again afterwards. This level of flexibility is important for fast and safe navigation within more complex environments in order to maximize the motion effectiveness. The flexibility is highlighted by dotted triangles, which represent the geometric configuration of the swarm in time. Let us call this flock geometry an α -lattice according to [45] and use it to represent a self-organizing structure, where individual inter-particle distances converge to a common value. This geometric configuration allows for small deviations from the expected structure (especially for particles in an environment with obstacles), which can be further quantified by *deviation energy* and can be used to evaluate the swarming model convergence. The deviation energy is derived in [45] and represents a non-smooth potential function of a set of particles, where the α -lattice configuration lies at its global minimum.

6.2. UVDAR in Control Feedback

To verify the feasibility of the complete system defined in figure 5, UVDAR vision-based mutual relative



(a) Flexible and effective navigation of a decentralized swarm of 5 UAVs through a 4 m wide narrow passage.

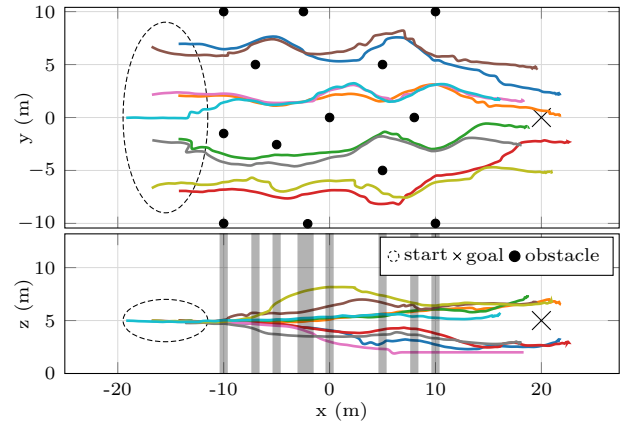


(b) Fast and efficient maneuvering of 6 UAVs emerging solely from local interactions during avoidance of a static obstacle.

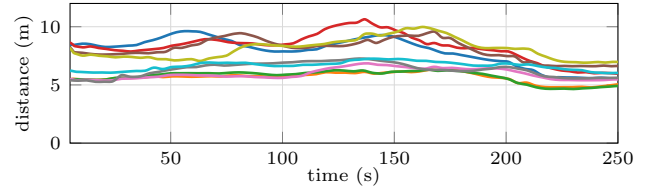
Figure 7: A fully-decentralized swarm of homogeneous units in a simulated 3D environment with static obstacles. The swarming model yields enough flexibility for the compact team to deviate from its aggregated structure in order to pass safely through a narrow gap (a) or to avoid an obstacle in an efficient and fast manner (b).

localization is deployed in the position control feedback loop of each homogeneous swarm agent. Throughout the experiment, the individual UAVs employ GNSS for self-state estimation. This is required to stabilize the flight of each dynamically unstable UAV mid-flight in a large open-space, where the swarm was deployed. However, the agents do not share any information through a communication network and instead they directly perceive the neighboring particles using UVDAR. The blinking frequencies of the UAVs (IDs) within the experiment were static and unique. This improves the performance of the UVDAR localization as unique IDs in the image stream help to separate occluded detections and track the units in time. To the best of our knowledge, this is the first deployment of a fully decentralized aerial swarming system in a real environment (outside laboratory-like conditions) with direct localization and with no communication or position sharing allowed.

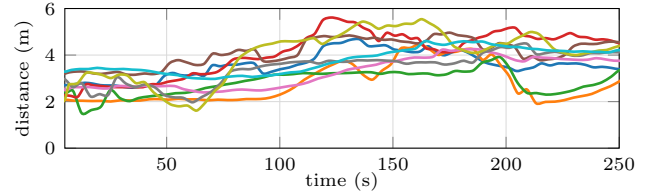
As explicitly shown in figure 10, use of a



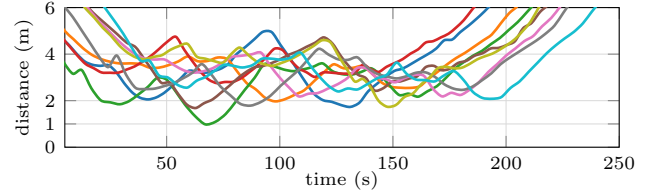
(a) Orthogonal views on the trajectories of the particles.



(b) Average distance amid the UAVs.



(c) Minimal distance amid the UAVs.



(d) Minimal distance to the closest obstacle.

Figure 8: Navigation of a decentralized swarm of 9 homogeneous UAVs in a forest-like environment with a high density of circular obstacles – tree trunks (a). The experiment showcases the cooperative steering within the environment and the emerging properties of mutual long-term cohesion (b), safe mutual separation (c), and reliable obstacle avoidance (d).

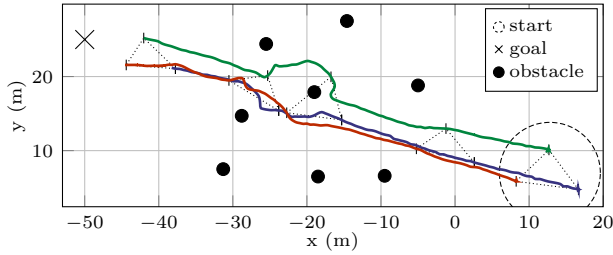
local sensing method maintains the abilities of the bio-inspired swarming model, namely self-organizing behavior, together with collision-free and cohered navigation. The swarm is capable of navigation throughout the environment in a compact structural constellation without any external interference to a sequence of global navigation goals. The figure shows the ability to preserve a compact structure emerging from local UVDAR-based perception (figure 2 and



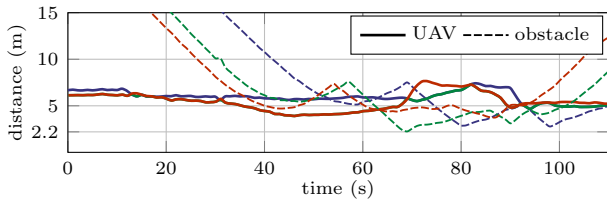
(a) Swarm of 3 UAVs navigating through an artificial forest.



(b) Onboard RGB view from one of the homogeneous units.



(c) Trajectories of individual UAVs (coded by color). The dotted triangles represent the swarm constellation (α -lattices) at a given time, which highlights the compactness and the flexibility of the swarm navigating amidst obstacles.



(d) Euclidean distance to the nearest UAV and obstacle for each swarm agent (coded by color). The minimum distance reached is 2.18 m.

Figure 9: Aerial swarm of 3 homogeneous UAVs in a real-world forest-like environment filled with artificial obstacles.

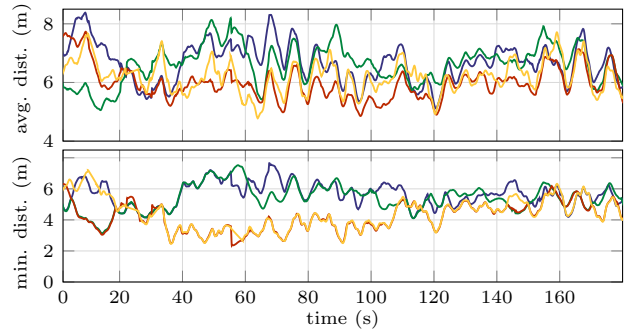
figure 3 show the perceived data of a single swarm agent in this particular experiment) and the elementary rules presented in section 4, while the homogeneous units do not share any information among themselves.

6.3. Analysis on Direct Observation Accuracy

In real-world conditions, all estimation subsystems are incorporated with various measurements containing a stochastic noise element. The origin of this stochastic part is of numerous types (e.g., vibrations, discretization, approximations, sensor non-linearity, time desynchronization, lack of motion compensation, or optical discrepancies) and most of these inaccuracies need to be accounted for. For example, the stabilization and control system of UAVs requires a continuous stream of inertial measurements to cope with hardware-based and synchronization inaccuracies, in order to stabilize the dynamically unstable system in mid-flight. The influence of these inaccuracies needs to



(a) Aerial view on the decentralized swarm of 4 UAVs (red) and a static reference to assist with the scale perception (blue).



(b) Average and minimal Euclidean distance among the homogeneous agents. The minimum distance reached is 2.04 m.

Figure 10: A fully-decentralized swarm of 4 homogeneous UAVs navigating through an obstacle-less environment with UVDAR integrated into the position control feedback, as outlined by the scheme in figure 5.

be carefully analyzed, and the results of the analyses must be incorporated into the design of a swarming model in order to compensate for the uncertainties of real-world systems.

As discussed in the review of the related literature (see section 1.1), dense robotic swarms candidly communicate either external positioning estimates or individual global state estimates amid the swarm units. In addition to the requirements of the communication infrastructure, this methodology imitates the bio-inspired design of mutual localization by establishing the relative relations from the global data. This incorporates the global self-localization error, and can lead to dangerous decision making, and also to communication-based failures. However, our approach imitates biological systems by relying solely on direct localization without the need for known global states of the neighbors or of the unit itself. This bounds the overall performance of the system solely to the accuracy of the direct localization. It entirely

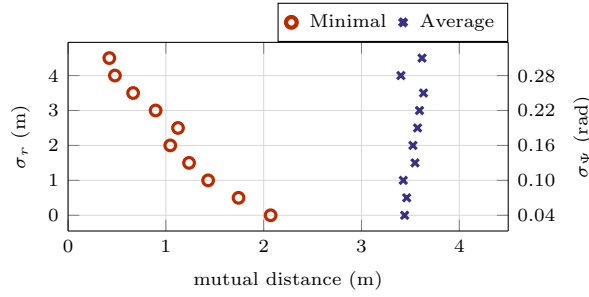


Figure 11: Dependency of the direct localization accuracy on the stability of an aerial swarm. The plot shows exponential decline of the minimum distance amid the swarm units with a growing degree of the localization error. The localization error is modeled as a multivariate normal distribution with uncorrelated zero-mean variables: the radial distance (standard deviation σ_r) and the relative azimuth (standard deviation σ_ψ).

removes the need for a communication infrastructure, and allows for full decentralization of the system architecture.

To analyze the impact of direct localization accuracy on the overall performance of our swarming framework, we present two inquiries: the influence of the error degree on the stability of a decentralized swarm, and the data-based accuracy of UVDAR in real-world conditions. As our focus applies to vision-based direct localization, the error of 3D relative localization can be expressed in spherical coordinates – radial distance, azimuth, and elevation – separately. Bear in mind that due to the vision-based nature of UVDAR discussed in section 3, the statistical characteristics of the elevation error are assumed to be identical with the azimuthal error. To maintain simplicity, the elevation error is therefore omitted from the presentation of the results.

The impact of a direct localization error on the stability of a swarm was analyzed on a set of computational simulations. A decentralized swarm of UAVs with simulated dynamics, control & state estimation disturbances, and sensory inaccuracies, was deployed in scenarios with various degrees of the direct localization error according to figure 11. Although the data show the minimum influence of the error on the average distance among the swarm units, the stochastic element induces oscillations of the mutual distances. These deviations from a consensual mutual distance arise directly from the inaccuracy of direct localization and from time-based and dynamics-based delays. This has a negative impact on the stability properties of the entire swarm, as shown by the exponential decline of the minimal distance amid the swarm units with the increasing degree of the radial distance and the relative azimuth error in figure 11. In real-world systems, a

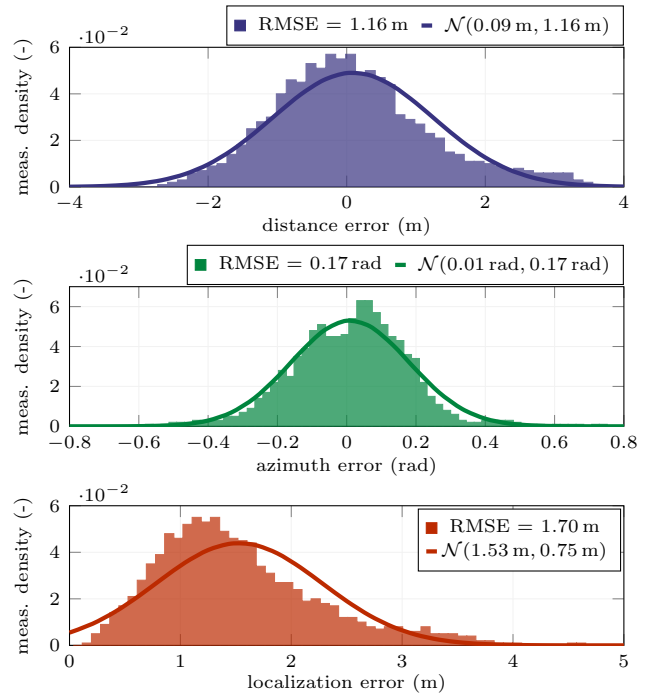
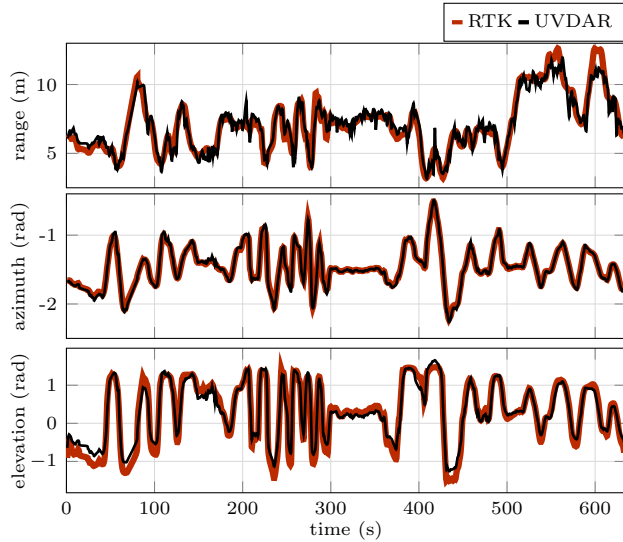


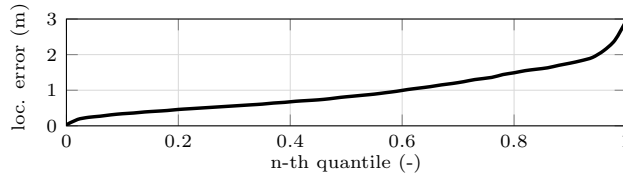
Figure 12: Quantitative accuracy of UVDAR direct localization with respect to GNSS positioning in real-world conditions. The figure shows error histograms and their normalized normal distribution $\mathcal{N}(\mu, \sigma)$ approximations of the directly estimated relative distance, the relative azimuth, and the global 3D position.

suitable swarm density must be thoroughly considered with respect to the accuracy and the reliability of the direct localization in order to prevent undesired collisions.

The accuracy of UVDAR in real-world conditions during the deployment of the decentralized swarm of 4 UAV units in an open environment (see figure 10) is expressed by the error histograms in figure 12. During this experiment, the self-localization of the individual UAVs was arranged by GNSS. The statistical analysis uses global positioning for a quantitative evaluation of the direct localization accuracy. Although global positioning yields a relatively high error, the state estimation module (see section 5) fuses this global state estimate with inertial measurements, which makes the output estimate robust towards sudden short-term changes. The positioning is still prone to long-term drift, which is minimal in terms of GNSS and therefore does not significantly impact the evaluation of the direct localization within a dense swarm. The fused global estimate is therefore used as ground truth data for the quantitative evaluation in figure 12. This evaluation on real-world data shows the ability of UVDAR to estimate the relative



(a) Relative localization represented by the spherical coordinates (expressed in the origin of the camera)



(b) Quantiles of the absolute 3D localization error

Figure 13: Real-world accuracy of UVDAR direct localization in a controlled environment — tracking of a single mid-flight UAV relative to a static ground UV camera. The UVDAR localization is compared to ground-truth data obtained with the use of RTK-GNSS. The absolute RMSE of the relative 3D localization in this experiment reached 1.11 m (the median is 0.81 m).

distance with 1.16 m root mean square error (RMSE) and the relative azimuth with RMSE of 0.17 rad. These separated errors then combine together with the elevation estimate to anticipate the relative 3D position of the neighboring particles within a moving aerial swarm with RMSE of 1.7 m.

The accuracy of UVDAR in real-world conditions is further analyzed in a controlled outdoor environment. During an independent experiment, a position of a single mid-air UAV was tracked in data from a static ground camera equipped with UVDAR and was compared to a precise RTK-GNSS (2 cm accuracy) serving as a ground-truth. The comparison of the relative localization with the ground-truth data is shown in figure 13. The data show the property of UVDAR to localize an aerial unit with RMSE of 1.11 m.

The concluded accuracy is particularly important for the design of bio-inspired systems employing the UVDAR sensor as a source of direct localization of neighboring units. The quantitative results of

this analysis allow for appropriate compensation of the inaccuracies and credible verification of swarming models in a simulator, which necessarily precede real-world applications.

7. Conclusion

This article has presented a framework for deploying fully-decentralized aerial swarms in real-world conditions with the use of vision-based UV mutual relative localization of neighboring swarm units. The framework architecture, as well as the off-the-shelf UVDAR system for direct localization within an aerial swarm, has been thoroughly discussed, has been deployed on a decentralized swarm of UAVs in real-world environments, and its performance has been analyzed. The experimental analysis verified the stability of UVDAR as an input into a fully-decentralized swarming architecture, which embodies the communication-free and local-information swarming models that are commonly found among biological systems. The set of real-world experiments is, to the best of our knowledge, the first deployment of a decentralized swarm of UAVs with no use of a communication network or of external localization. The system is provided as open source, and is designed for simple integration and verification of flocking techniques (often bio-inspired), respecting the requirements of the swarming paradigm.

Acknowledgments

This work was supported by the Czech Science Foundation (GAČR) under research project No. 20-10280S, by CTU grant no SGS20/174/OHK3/3T/13, by funding from the European Union's Horizon 2020 research and innovation programme under grant agreement No. 871479, and by OP VVV project CZ.02.1.01/0.0/0.0/16 019/0000765 "Research Center for Informatics". The authors thank Daniel Heřt for preparing all the necessary equipment required for the experimental analysis.

Supplementary Materials

The multimedia materials supporting the article are available at <http://mrs.felk.cvut.cz/research/swarm-robotics>. The entire system is also available as open source at <https://github.com/ctu-mrs>.

ORCID

Pavel Petráček : 0000-0002-0887-9430
 Viktor Walter : 0000-0001-8693-6261
 Tomáš Báča : 0000-0001-9649-8277
 Martin Saska : 0000-0001-7106-3816

References

- [1] Štibinger P, Báča T and Saska M 2020 Localization of Ionizing Radiation Sources by Cooperating Micro Aerial Vehicles with Pixel Detectors in Real-Time *IEEE Robot. Autom. Lett.* **5** 3634–3641
- [2] Gassner M, Cieslewski T and Scaramuzza D 2017 Dynamic collaboration without communication: Vision-based cable-suspended load transport with two quadrotors *Int. Conf. on Robotics and Automation* pp 5196–5202
- [3] Trianni V 2008 *Evolutionary Swarm Robotics: Evolving Self-Organising Behaviours in Groups of Autonomous Robots (Studies in Computational Intelligence)* 1st ed (Springer Publishing Company, Incorporated)
- [4] Young G F, Scardovi L, Cavagna A, Giardina I and Leonard N E 2013 Starling Flock Networks Manage Uncertainty in Consensus at Low Cost *PLOS Computational Biology* **9** 1–7
- [5] Chung S, Paranjape A A, Dames P, Shen S and Kumar V 2018 A Survey on Aerial Swarm Robotics *IEEE Trans. Robot.* **34** 837–855
- [6] Nguyen T, Qiu Z, Nguyen T H, Cao M and Xie L 2019 Distance-Based Cooperative Relative Localization for Leader-Following Control of MAVs *IEEE Robot. Autom. Lett.* **4** 3641–3648
- [7] Bhavana T, Nithya M and Rajesh M 2017 Leader-follower co-ordination of multiple robots with obstacle avoidance *SmartTechCon*
- [8] Saska M, Báča T, Thomas J, Chudoba J, Přeučil L, Krajník T, Faigl J, Loianno G and Kumar V 2017 System for deployment of groups of unmanned micro aerial vehicles in GPS-denied environments using onboard visual relative localization *Auton. Robot.* **41** 919–944
- [9] Faigl J, Krajník T, Chudoba J, Přeučil L and Saska M 2013 Low-cost embedded system for relative localization in robotic swarms *Int. Conf. on Robotics and Automation* pp 993–998
- [10] De Silva O, Mann G K I and Gosine R G 2015 An Ultrasonic and Vision-Based Relative Positioning Sensor for Multirobot Localization *IEEE Sensors J.* **15** 1716–1726
- [11] Yan X, Deng H and Quan Q 2019 Active Infrared Coded Target Design and Pose Estimation for Multiple Objects *Int. Conf. on Intelligent Robots and Systems* pp 6885–6890
- [12] Censi A, Strubel J, Brandli C, Delbruck T and Scaramuzza D 2013 Low-latency localization by active LED markers tracking using a dynamic vision sensor *Int. Conf. on Intelligent Robots and Systems* pp 891–898
- [13] Park H, Choi I, Park S and Choi J 2013 Leader-follower formation control using infrared camera with reflective tag *10th Int. Conf. on Ubiquitous Robots and Ambient Intelligence* pp 321–324
- [14] Chaudhary K, Zhao M, Shi F, Chen X, Okada K and Inaba M 2017 Robust real-time visual tracking using dual-frame deep comparison network integrated with correlation filters *Int. Conf. on Intelligent Robots and Systems* pp 6837–6842
- [15] Carrio A, Tordesillas J, Vemprala S, Saripalli S, Campoy P and How J P 2020 Onboard Detection and Localization of Drones Using Depth Maps *IEEE Access* **8** 30480–30490
- [16] Intel® 2019 Drones Light Up The Sky URL [intel.com/content/www/us/en/technology-innovation/aerial-technology-light-show.html](https://www.intel.com/content/www/us/en/technology-innovation/aerial-technology-light-show.html)
- [17] Virágh C, Vásárhelyi G, Tarcai N, Szörényi T, Somorjai G, Nepusz T and Vicsek T 2014 Flocking algorithm for autonomous flying robots *Bioinspir. Biomim.* **9** 025012
- [18] Vásárhelyi G, Virágh C, Somorjai G, Tarcai N, Szörényi T, Nepusz T and Vicsek T 2014 Outdoor flocking and formation flight with autonomous aerial robots *Int. Conf. on Intelligent Robots and Systems* pp 3866–3873
- [19] Vásárhelyi G, Virágh C, Somorjai G, Nepusz T, Eiben A E and Vicsek T 2018 Optimized flocking of autonomous drones in confined environments *Sci. Robot.* **3**
- [20] EHang 2019 EHang Drone Formation Flight URL ehang.com/formation
- [21] Hauert S, Leven S, Varga M, Ruini F, Cangelosi A, Zufferey J and Floreano D 2011 Reynolds flocking in reality with fixed-wing robots: Communication range vs. maximum turning rate *Int. Conf. on Intelligent Robots and Systems* pp 5015–5020
- [22] Bürkle A, Segor F and Kollmann M 2011 Towards Autonomous Micro UAV Swarms *J. Intell. Robot. Syst.* **61** 339–353
- [23] Kushleyev A, Mellinger D, Powers C and Kumar V 2013 Towards A Swarm of Agile Micro Quadrotors *Auton. Robot.* **35** 287–300
- [24] Weinstein A, Cho A, Loianno G and Kumar V 2018 Visual Inertial Odometry Swarm: An Autonomous Swarm of Vision-Based Quadrotors *IEEE Trans. Robot. Autom.* **3** 1801–1807
- [25] Stirling T, Roberts J, Zufferey J C and Floreano D 2012 Indoor navigation with a swarm of flying robots *Int. Conf. on Robotics and Automation* 4641–4647
- [26] Nägeli T, Conte C, Domahidi A, Morari M and Hilliges O 2014 Environment-independent formation flight for micro aerial vehicles *Int. Conf. on Intelligent Robots and Systems* pp 1141–1146
- [27] van Diggelen F and Enge P K 2015 The World’s first GPS MOOC and Worldwide Laboratory using Smartphones *ION GNSS+* pp 361–369
- [28] Garcia Carrillo L R, Fantoni I, Rondon E and Dzul A 2015 Three-dimensional position and velocity regulation of a quad-rotorcraft using optical flow *IEEE Trans. Aerosp. Electron. Syst.* **51** 358–371
- [29] Schmid K, Lutz P, Tomić T, Mair E and Hirschmüller H 2014 Autonomous Vision-based Micro Air Vehicle for Indoor and Outdoor Navigation *J. Field Robot.* **31** 537–570
- [30] Kohlbrecher S, Meyer J, von Stryk O and Klingauf U 2011 A Flexible and Scalable SLAM System with Full 3D Motion Estimation *Int. Symp. on Safety, Security and Rescue Robotics* pp 155–160
- [31] Schmickl T and Hamann H 2016 *BEECLUST: A swarm algorithm derived from honeybees: Derivation of the algorithm, analysis by mathematical models, and implementation on a robot swarm* pp 95–137
- [32] Bodi M, Möslinger C, Thenius R and Schmickl T 2015 BEECLUST used for exploration tasks in Autonomous Underwater Vehicles *8th Int. Conf. on Mathematical Modelling* pp 819–824
- [33] Shah D and Vachhani L 2019 Swarm Aggregation Without Communication and Global Positioning *IEEE Trans. Robot. Autom.* **4** 886–893
- [34] Olaronke, Iroju and Ikono, Rhoda and Gambo, Ishaya and Ojerinde, Oluwaseun 2020 A Systematic Review of Swarm Robots *Current Journal of Applied Science and Technology* **39** 79–97
- [35] Oh H, Shirazi A R, Sun C and Jin Y 2017 Bio-inspired self-organising multi-robot pattern formation: A review *Rob. Auton. Syst.* **91** 83–100
- [36] Smith N M, Dickerson A K and Murphy D 2019 Organismal aggregations exhibit fluidic behaviors: a review *Bioinspir. Biomim.* **14** 031001
- [37] Saska M, Vakula J and Přeučil L 2014 Swarms of Micro Aerial Vehicles Stabilized Under a Visual Relative Localization *Int. Conf. on Robotics and Automation* pp 3570–3575
- [38] Walter V, Staub N, Saska M and Franchi A 2018 Mutual

- Localization of UAVs based on Blinking Ultraviolet Markers and 3D Time-Position Hough Transform *14th Int. Conf. on Automation Science and Engineering* pp 298–303
- [39] Walter V, Staub N, Franchi A and Saska M 2019 UVDAR System for Visual Relative Localization With Application to Leader–Follower Formations of Multirotor UAVs *IEEE Trans. Robot. Autom.* **4** 2637–2644
- [40] Walter V, Vrba M and Saska M 2020 On training datasets for machine learning-based visual relative localization of micro-scale UAVs *Int. Conf. on Robotics and Automation* Accepted
- [41] International Commission on Non-Ionizing Radiation Protection and others 2004 Guidelines on limits of exposure to ultraviolet radiation of wavelengths between 180 nm and 400 nm (incoherent optical radiation) *Health Physics* **87** 171–186
- [42] ProLight Opto Technology Corporation 2013 ProLight PM2B-1LLE 1W UV Power LED Technical Datasheet
- [43] Calovi D S, Lopez U, Ngo S, Sire C, Chaté H and Theraulaz G 2014 Swarming, schooling, milling: phase diagram of a data-driven fish school model *New J. Phys.* **16** 015026
- [44] Reynolds C W 1987 Flocks, Herds and Schools: A Distributed Behavioral Model *14th Ann. Conf. on Computer Graphics and Interactive Techniques* pp 25–34
- [45] Olfati-Saber R 2006 Flocking for multi-agent dynamic systems: algorithms and theory *IEEE Trans. Autom. Control* **51** 401–420
- [46] Zhu H, Juhl J, Ferranti L and Alonso-Mora J 2019 Distributed Multi-Robot Formation Splitting and Merging in Dynamic Environments *Int. Conf. on Robotics and Automation* 9080–9086
- [47] Erunsal I K, Ventura R and Martinoli A 2019 Nonlinear Model Predictive Control for 3D Formation of Multirotor Micro Aerial Vehicles with Relative Sensing in Local Coordinates **arXiv:1904.03742**
- [48] Curiac D I and Volosencu C 2015 Imparting protean behavior to mobile robots accomplishing patrolling tasks in the presence of adversaries *Bioinspir. Biomim.* **10** 056017
- [49] Elamvazhuthi K and Berman S 2019 Mean-field models in swarm robotics: a survey *Bioinspir. Biomim.* **15** 015001
- [50] Alonso-Mora J 2014 Collaborative motion planning for multi-agent systems *Ph.D. thesis* (Autonomous Systems Lab, ETH-Zürich)
- [51] Mohamed E F, El-Metwally K and Hanafy A R 2011 An improved Tangent Bug method integrated with artificial potential field for multi-robot path planning *Int. Symp. on Innovations in Intelligent Systems and Applications* pp 555–559
- [52] Báča T, Petrлік M, Vrba M, Spurný V, Pěnička R, Heřt D and Saska M 2020 The MRS UAV System: Pushing the Frontiers of Reproducible Research, Real-world Deployment, and Education with Autonomous Unmanned Aerial Vehicles **arXiv:2008.08050**
- [53] Lee T, Leok M and McClamroch N H 2010 Geometric tracking control of a quadrotor UAV on SE(3) *49th Conf. on Decision and Control* pp 5420–5425
- [54] Petráček P, Krátký V and Saska M 2020 Dronument: System for Reliable Deployment of Micro Aerial Vehicles in Dark Areas of Large Historical Monuments *IEEE Trans. Robot. Autom.* **5** 2078–2085
- [55] Báča T, Hert D, Loianno G, Saska M and Kumar V 2018 Model Predictive Trajectory Tracking and Collision Avoidance for Reliable Outdoor Deployment of Unmanned Aerial Vehicles *Int. Conf. on Intelligent Robots and Systems* pp 6753–6760
- [56] Meier L, Tanskanen P, Heng L, Lee G H, Fraundorfer F and Pollefeys M 2012 PIXHAWK: A Micro Aerial Vehicle Design for Autonomous Flight Using Onboard Computer Vision *Auton. Robots* **33** 21–39
- [57] Koenig N and Howard A 2004 Design and use paradigms for Gazebo, an open-source multi-robot simulator *Int. Conf. on Intelligent Robots and Systems* vol 3 pp 2149–2154
- [58] Stanford Artificial Intelligence Laboratory et al Robot Operating System URL ros.org